

Density, heterogeneity and deformability of red cells as markers of clinical severity in hereditary spherocytosis

Rick Huisjes,¹ Asya Makhro,² Esther Llaudet-Planas,³ Laura Hertz,⁴ Polina Petkova-Kirova,⁴ Liesbeth P. Verhagen,¹ Silvia Pignatelli,¹ Minke A.E. Rab,¹ Raymond M. Schiffelers,¹ Elena Seiler,² Wouter W. van Solinge,¹ Joan-LLuis Vives Corrons,³ Lars Kaestner,^{4,5} Maria Mañú-Pereira,⁶ Anna Bogdanov² and Richard van Wijk¹

¹Department of Clinical Chemistry and Hematology, University Medical Center Utrecht, Utrecht University, Utrecht, the Netherlands; ²Red Blood Cell Research Group, Institute of Veterinary Physiology, Vetsuisse Faculty and the Zurich Center for Integrative Human Physiology (ZIHP), University of Zurich, Zurich, Switzerland; ³Red Blood Cell Defects and Hematopoietic Disorders Unit, Josep Carreras Leukemia Research Institute, Badalona, Barcelona, Spain; ⁴Theoretical Medicine and Biosciences, Medical Faculty, Saarland University, Homburg/Saar, Germany; ⁵Experimental Physics, Saarland University, Saarbruecken, Germany and ⁶Rare Anemia Research Unit. Vall d'Hebron Research Institution, University Hospital Vall d'Hebron, Barcelona, Spain

©2020 Ferrata Storti Foundation. This is an open-access paper. doi:10.3324/haematol.2018.188151

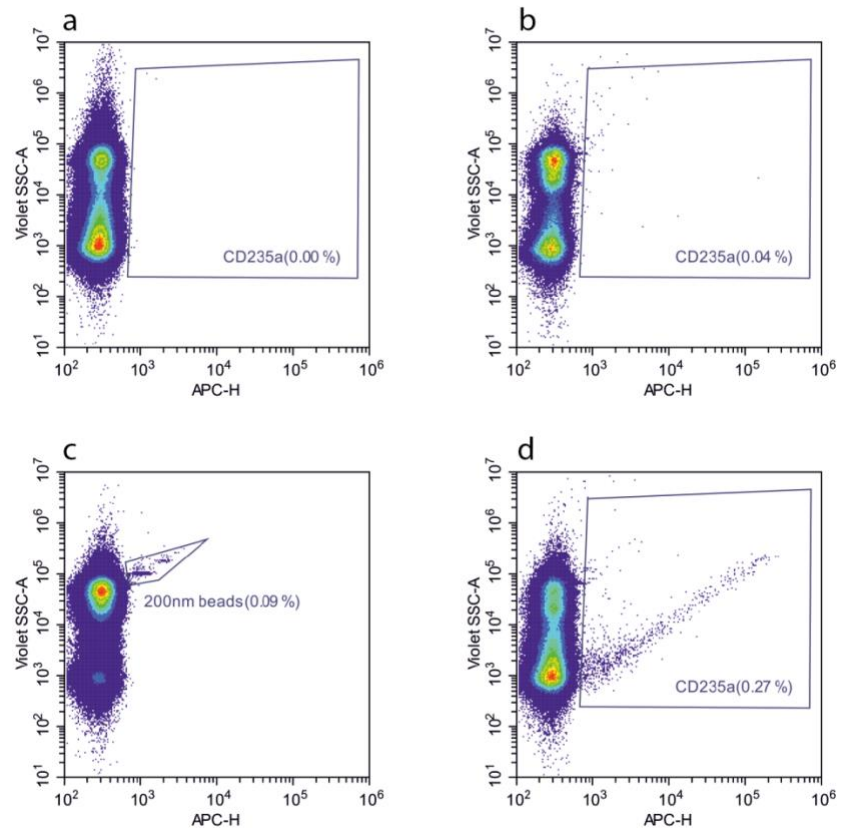
Received: April 3, 2018.

Accepted: May 28, 2019.

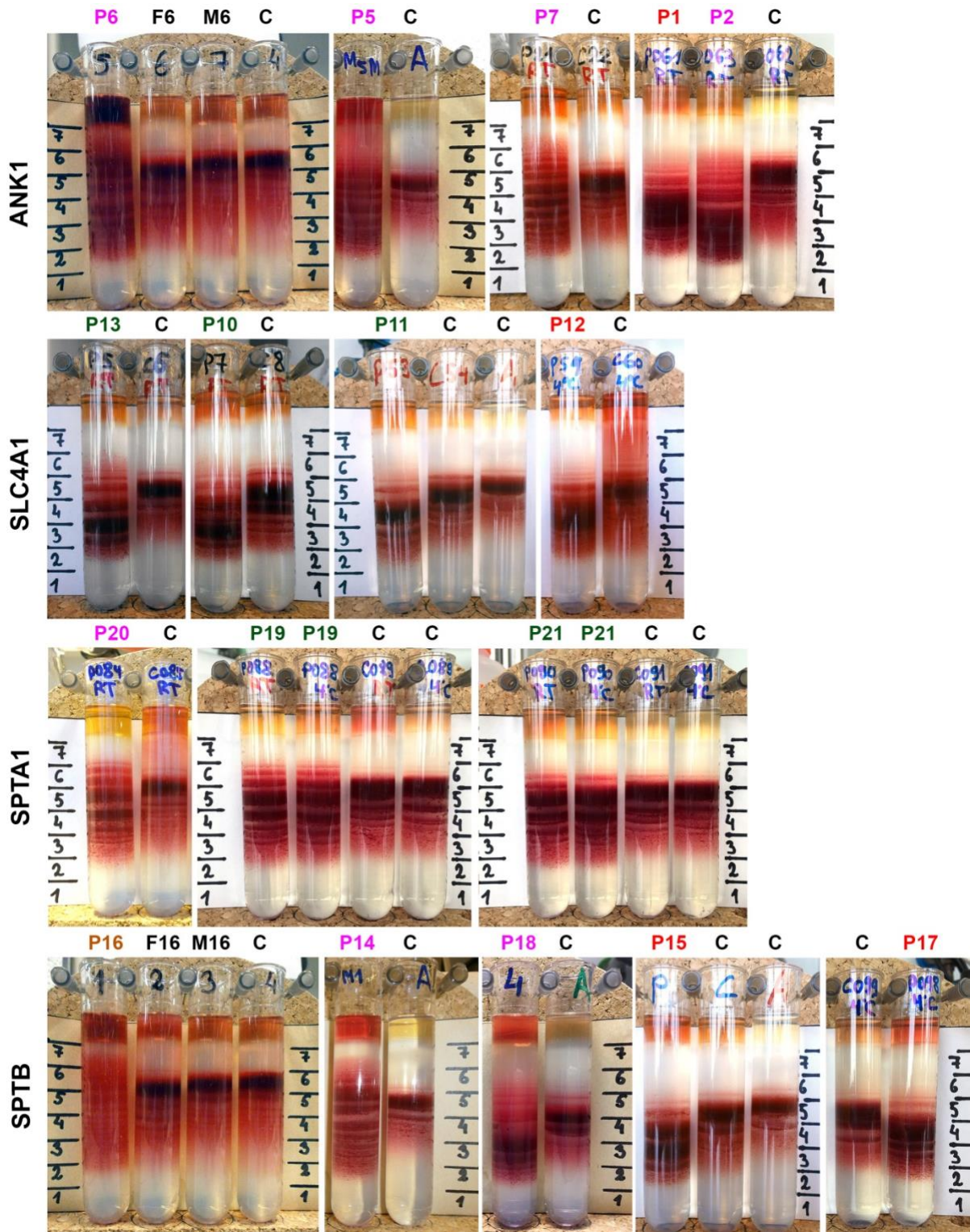
Pre-published: May 30, 2019.

Correspondence: *RICHARD VAN WIJK* - r.vanWijk@umcutrecht.nl

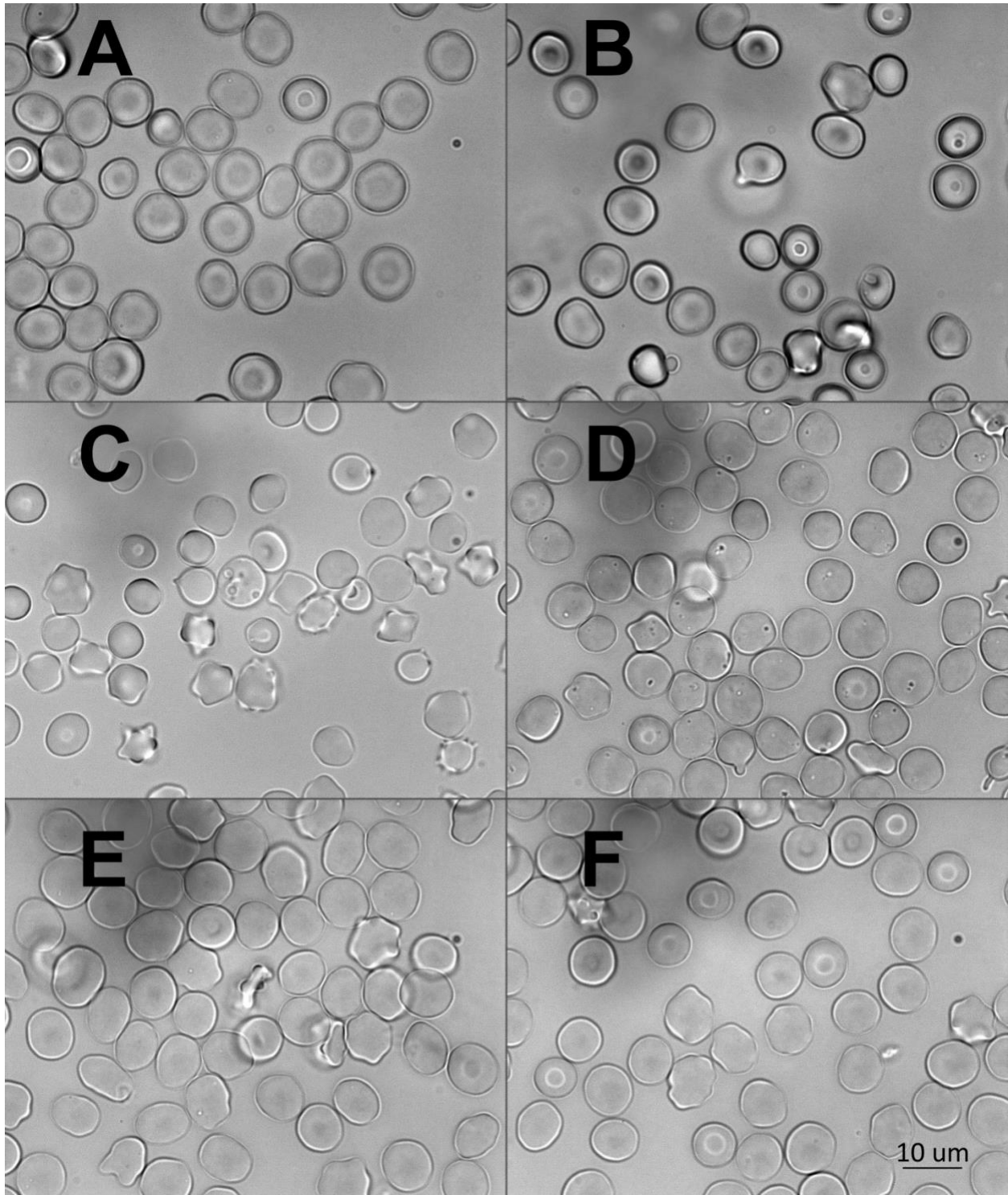
Supplemental Figures and Tables



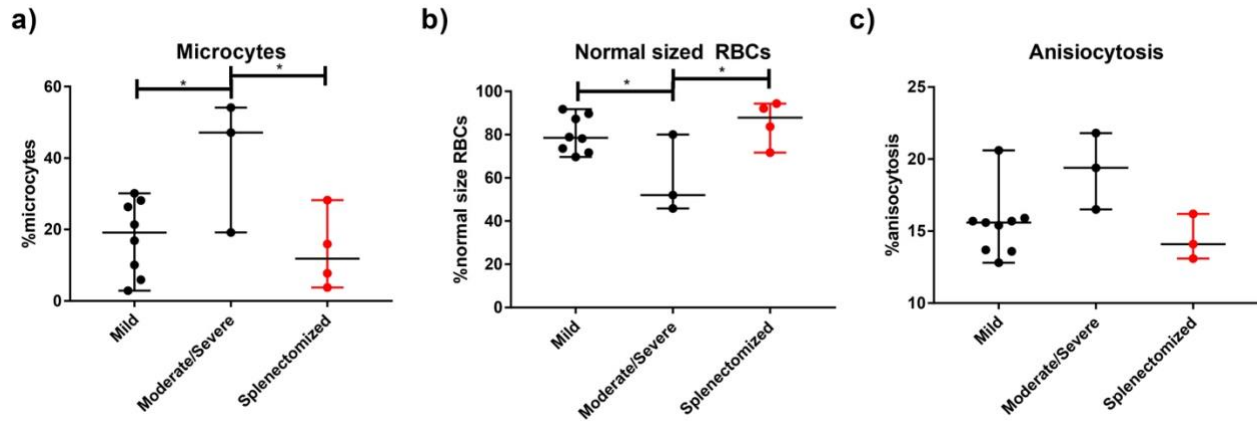
S.Fig 1: Panel a, b, c and d indicate gating strategies to detect RBC vesicles in plasma. A) Patient plasma diluted in PBS b) CD235a-APC diluted in PBS c) 200nm Ultra Rainbow Fluorescent Beads (Spherotech, Inc.) diluted in PBS d) representative APC-H vs. Violet plot of patient sample (plasma + CD235a-APC).



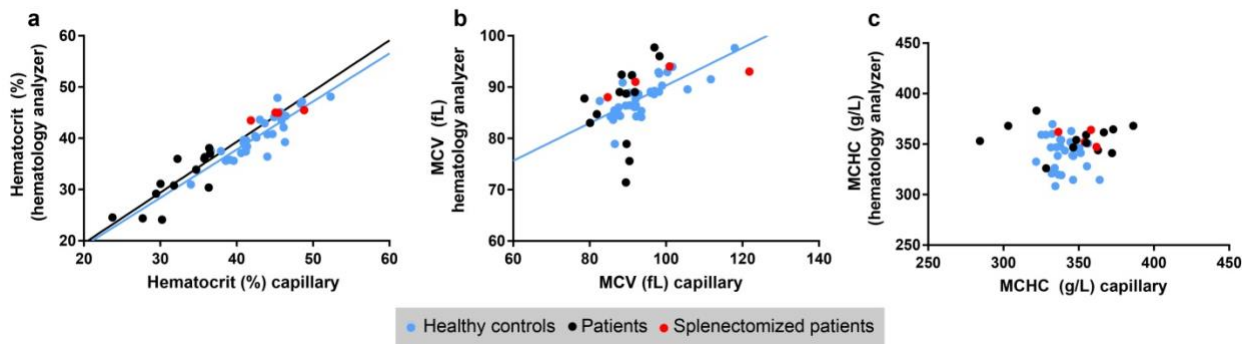
S.Fig 2: HS RBCs separated on the 90% Percoll density gradient compared to co-transported controls. Mild clinical severity is marked in dark-green, moderate – in pink, severe - in orange, splenectomized – in red, controls and unaffected relatives marked in black. F - father of the patient, M – mother of the patient. Control blood sample to P12 was partially frozen during the transportation.



S.Fig 3: Representative life images of RBC resuspended in plasma-like buffer. A – cells from P19, mild anemia, B – cells from P7, moderate anemia, C – cells from P2, severe anemia, D – cells from splenectomized P1, E and F – cells from two co-transported controls.



S.Fig 4: %microcytes, %normal sized RBCs and %anisocytosis in mild, moderate/severe and splenectomized HS measured by digital microscopy.



S.Fig 5: correlations between automated and capillary measurements of hematocrit, MCV and MCHC. In blue dots healthy controls, black dots HS patients and red dots splenectomized HS patients dots patient are depicted. Statistical significant correlations are displayed with linear regression lines. a) correlations between automated hematocrit and capillary hematocrit measurements b) correlations between automated MCV and capillary MCV measurements, d) correlations between automated MCHC and capillary MCHC measurements

Supplemental methods

Subjects

Patients diagnosed with HS were enrolled in the CoMMiTMenT-study (<http://www.rare-anaemia.eu/>) after spoken and written informed consent. This study was approved by the Medical Ethical Research Board of the University Medical Center Utrecht, the Netherlands, (UMCU) under reference code 15/426M 'Disturbed ion homeostasis in hereditary haemolytic anaemia' and by the Ethical Committee of Clinical Investigations of Hospital Clinic, Spain, (IDIBAPS) under the reference code 2013/8436. HS patients were included in the study after confirming the diagnosis of HS with gold standard techniques (i.e. osmotic gradient ektacytometry, osmotic fragility test, EMA-binding, microscopy¹) and DNA analysis by Next Generation Sequencing. In brief, seven genes commonly associated with RBC membrane disorders were analyzed: *SPTA1* (a-spectrin), *SPTB* (b-spectrin), *ANK1* (ankyrin), *SLC4A1* (Band 3), *EPB41* (protein 4.1), *EPB42* (protein 4.2), and *RHAG* (Rhesus-associated glycoprotein). After enrichment of genomic DNA, using a custom Agilent SureSelectXT probe kit, protein coding and flanking intronic sequences were determined using a SOLID™-5500XL system. Variants were identified using an 'in house' developed NGS mapping and calling pipeline, and the Cartagenia BENCHlab NGS module was used for filtering and prioritization of possible pathogenic variants. Detected mutations were confirmed by conventional Sanger sequencing. Novel variants with a clear pathogenic nature (i.e. frameshift mutants, nonsense mutants, splice site mutations) were considered to be causal. All novel missense variants were tested for pathogenicity using commonly known prediction tools SIFT, PolyPhen-2, and MutationTaster. In addition, their occurrence in the healthy control population was investigated using Gnomad (<http://gnomad.broadinstitute.org>). Exclusion criteria were the use of erythrocyte transfusion in the last 90 days, age lower than three years and body weight lower than 18kg. After inclusion, HS patients were categorized to their genetic defect (i.e. *ANK1*, *SLC4A1*, *SPTA1* and *SPTB*) and to their clinical severity. Clinical severity in non-splenectomized HS patients was previously defined by Bolton-Maggs² on basis of

1) hemoglobin and 2) reticulocytes levels. Mild HS was defined as hemoglobin levels between 110–150 g/L, moderate HS as hemoglobin levels between 80–120 g/L and severe HS as hemoglobin levels lower than 80 g/L. HS patients with hemoglobin levels between 110 and 120 were categorized as mild or moderate on basis of their reticulocytes levels (i.e. lower or higher than 6% reticulocytes). Blood from healthy controls was anonymously obtained using the approved medical ethical protocol of 07/125 Mini Donor Dienst. Patient blood was shipped with blood from a healthy control overnight from the University Medical Center Utrecht (Utrecht, The Netherlands) and Institut d'Investigacions Biomèdiques August Pi i Sunyer/ Hospital Clínic de Barcelona (Barcelona, Spain) to Saar University (Homburg, Germany) and University of Zurich (Zurich, Swiss) in lithium-heparin tubes either at room temperature or at 4°C to perform advanced research tests³. Functional domains and protein lengths are obtained from Lux *et al.*, Satchwell *et al.*, Ding *et al.*, Barneaud-Rocca *et al.*, Yasunaga *et al.*, Bennett *et al.*^{4–9} and UniProt database (www.uniprot.org).

Hemocytometry analysis

Hemocytometry parameters (i.e. Hb, RBC numbers, hematocrit, MCV, MCH, MCHC, reticulocytes) were analyzed on the Abbott Sapphire cell analyzer (Abbott Diagnostics Division, Santa Clara, CA, USA) and ADVIA 2120 (Hematology System, Siemens Healthcare Diagnostics, Forchheim, Germany)

Capillary-based measurements of MCV and MCHC

Automated hematology measurements for hematocrit, MCV and MCHC can be affected various factors such as by shape, cell orientation and osmotic fragility¹⁰ and therefore were also measured by micro-capillaries. Also, we used capillary-based measurements of MCV and MCHC, because RBC density measurements by Percoll are known to correlate with RBC age¹¹. Hematocrit (hct) capillaries were filled with intact well-mixed heparinized blood samples. For each blood sample, hematocrit measurements were carried out in triplicate. Capillaries were centrifuged for 5 min at 12.000 rpm (Hematocrit 20,

Hettich Zentrifugen). The total height of the samples and packed RBC height in capillary was measured manually with 0.1 mm accuracy. Mean hematocrit was calculated for the triplicate measurements and an average hematocrit was taken. MCV was calculated using the formula; $MCV = \text{hematocrit} / [\text{RBC number}]$ and MCHC was calculated using the formula; $MCHC = [\text{Hemoglobin}]/\text{Hematocrit}$.

Intracellular potassium measurements

An aliquot lithium-heparin whole blood was directly stored at -80°C after blood collection. At the same time, an aliquot of lithium heparin plasma was obtained by centrifugation of whole blood at 1000g for 10 minutes. The obtained plasma was centrifuged again at 4000g for 10 minutes to remove debris and residual cells. At the day of analysis, the aliquot of whole blood underwent two additional freeze-thaw cycles in liquid nitrogen to ensure complete lysis. The hemolyzed whole blood and plasma samples were measured using the Instrumentation Laboratory IL943 Flame Photometer. Intracellular potassium ($[K^+]_{RBC}$) was calculated using the following formula;

$$[K^+]_{RBC} = \frac{[K^+]_{\text{whole blood}} - ([K^+]_{\text{plasma}} * (1 - \text{hematocrit}))}{\text{hematocrit}}$$

Pre-incubated osmotic fragility test and eosin-5-maleimide binding

For the osmotic fragility test, lithium heparinized whole blood was incubated for 24 hours at 37°C. Incubated whole blood was subsequently added to different concentrations of NaCl (pH=7.4) (Range 1.0 – 12.0 g/L). After 30 minutes of incubation, RBCs were spun down at 1250g for 5 minutes. The absorbance of the supernatants were measured at 540nm using a Spectramax ME2. Eosin-5-maleimide (EMA) binding was determined according to previously published protocols¹²⁻¹⁴. Briefly, washed RBCs were incubated with 0.5 mg/ml eosin-5-maleimide and measured using the BD FACSCanto®. FITC signals

of EMA-bound RBCs from patients were percentual related to the average of EMA-signals from 6 healthy controls per measurement.

Osmotic gradient ektacytometry

Osmotic gradient ektacytometry measurements of RBCs from healthy controls and HS patients were obtained using the Osmoscan module on the Lorrca MaxSis (Mechatronics, The Zwaag, The Netherlands). 250 μ L of whole blood was standardized to a hemoglobin concentration of 12.9 g/dL and injected in 5ml isotonic polyvinylpyrrolidone (PVP), and osmotic gradient ektacytometry was further carried out as previously described¹⁵⁻¹⁷. Briefly, RBCs are subjected to constant shear stress (30 Pa.S) while the osmolarity gradually increases from \approx 80 mOsmol/L to \approx 550 mOsmol/L. During this increase in osmolarity, a refraction pattern is generated by a laser and this pattern is captured by camera. The accompanied software measures the elongation index (EI), which is calculated by $EI=(a-b)/(a+b)$. In this formula, a represents the length and b the width of the RBC population as observed in the refraction pattern. Representative osmotic gradient ektacytometry curves are depicted in grey in Fig 3a-d. In the osmotic gradient ektacytometry curve, three characteristic points are depicted. 1) EI_{max} represents the maximal deformability of the RBC population and is found whereas EI is maximal. 2) O_{hyper} (in mOsmol/L) represents the intracellular viscosity (or RBC density, or RBC hydration state) and is found at the hypertonic axis where the EI is 50% of EI_{max} . Lower values of O_{hyper} indicate increased intracellular viscosity and denser RBCs. 3) O_{min} (in mOsmol/L) correlates with the 50% lysis point in the manual OFT and is found at hypotonic conditions whereas EI_{min} is minimal. Higher values of O_{min} indicates increased osmotic fragility (or decreased osmotic resistance).

Separation on the Percoll density gradient

Intact blood samples (1 ml each) were layered over the 12 ml of 90% Percoll solution containing plasma-like components (mM) 140 NaCl, 4 KCl, 0.75 MgCl₂, 2 CaCl₂, 0.015 ZnCl₂, 0.2 alanine, 0.2 glutamate-Na, 0.2 glycine, 0.1 arginine, 0.6 glutamine, 10 glucose, 20 HEPES-imidazole, pH 7.40 RT, 0.1% BSA. Percoll density gradient and RBC separation were performed during the centrifugation at 50.000g for 15 min, no brakes (Sorvall RC 5C plus, rotor SM-24). To avoid RBC volume artefacts related to the cold-induced inhibition of Na/K pump, centrifugation was performed at 30-36°C temperature interval.

Tubes with the RBC separated within the Percoll density gradient were photographed in front of the homogeneous light source. Images were automatically analyzed by the Visio 4D software (Arivis AG) as follows: RBC density distribution profile within the tube was produced. From the density profile, several parameters describing each blood sample were determined. The density profile was divided in a fraction with young cells, medium cells (also defined as M fraction) and dense cells. Within the M fraction the number of RBC populations were counted and average RBC density was determined. The average RBC density was defined as the location of the most intense RBC fraction (a.u.) relative to total length of the Percoll gradient.

RBC production, heterogeneity and turn-over rate markers

CD71 was measured to investigate the effects of RBC turn-over and reticulocytosis on RBC density parameters, as CD71 is a marker of (early) reticulocytes and erythroblasts. CD71 on RBCs was measured using flow cytometry. Blood was resuspended in plasma-like media with pH=7.4 (in 10mM HEPES, 120mM NaCl, 5mM KCl, 2mM CaCl₂, 0.8mM MgCl₂). RBCs were incubated with mouse anti-human CD71-FITC (eBiosciences, clone OKT9). FITC IgG1 isotype control antibody was used from eBiosciences.

Samples were measured using a BD FACS Canto II. HbA1c levels were measured in order to acquire information about RBC clearance¹⁸. HbA1c levels were measured using the Menarini/ARKRAY HA-8180V

RBC vesicles measurements

RBC vesicles in plasma were measured using a new generation flow cytometer, because RBC vesiculation is considered to increase RBC density and to cause the reduced surface-area-to-volume in HS¹⁹⁻²¹. Blood for RBC vesicle analysis was collected in CDPA (citrate phosphate dextrose adenine) additive solution³. Plasma was pipetted to new clean tubes after centrifugation for 10 minutes at 1000g. Cell debris and residual cells were removed from plasma after an additional centrifugation step (10 min, 4000g) and plasma was subsequently aliquoted and stored at -80°C awaiting for further analysis. RBC vesicles were measured using the Beckman Coulter CytoFLEX flow cytometer. RBC vesicles were stained with 50µg/ml mouse anti-human CD235a-APC (BD Biosciences) with an equal volume of 25 times diluted CDPA plasma in 0.2µM filtered PBS. After incubation in the dark for 30 minutes, samples were additionally 40 times diluted in 0.2µM filtered PBS and measured by flow cytometry for 6 minutes with a flow speed of 10µL/min. RBC vesicles were measured using SSC-violet-H vs. APC-H (allophycocyanin-H), and thresholds were set using blanks, plasma dilution samples with anti IgG2bk-APC and 200nm Ultra Rainbow Fluorescent Beads (Spherotech, Inc.), see S.Fig 1. Events positive for APC-H were considered to be RBC-vesicles. RBC-vesicle concentrations were standardized to RBC numbers in blood (particles/10¹² RBC/L plasma).

RBC morphology evaluation with light microscopy and digital microscopy

1,5 – 2 µl of intact blood was resuspended in 1 ml of plasma-like buffer containing 0.1% of bovine serum albumin. Then cell suspension was pipetted inside the microscopy chamber with the glass bottom. Cells were allowed to precipitate for 5-7 min and then microscopy images were taken by Zeiss Axiovert

inverted microscope using 100x objective.

Statistical analysis and correlations

Statistical analysis was carried out using Graphpad Prism 7.02 and IBM SPSS Statistics 21. One-Way ANOVA with Post-Hoc correction (Tukey) was used to test for significant differences between healthy controls and HS patients. Also, HS patients with different genotypes were tested to each other and to healthy controls. Significant levels of $P \leq 0.05$ were considered to reflect significant differences. In figures and figure legends significant differences are more specifically noted with * ($P \leq 0.05$), † ($P \leq 0.01$) or ‡ ($P \leq 0.001$). Reference values are depicted in gray and were obtained from laboratory references values or calculated using $\text{mean} \pm (1.96 * \text{SD})$ in healthy controls. Correlations were fitted with linear regression and correlations were considered significant when $P \leq 0.05$. Genotype-phenotype correlations were only carried out for unsplenectomized HS patients (Fig 3). In addition, in all figures splenectomized patients are depicted with red dots and were analyzed separately. Fisher's Exact Test was carried whether the phenotypes mild and moderate/severe were equally distributed along the different genotypes (*ANK1*, *SLC4A1*, *SPTB*, *SPTA1*). For Fisher's Exact Test we categorized the splenectomized patients as moderate/severe.

Reference list supplemental figures and methods

1. Bianchi P, Fermo E, Vercellati C, et al. Diagnostic power of laboratory tests for hereditary spherocytosis: a comparison study in 150 patients grouped according to molecular and clinical characteristics. *Haematologica* 2012;97(4):516–23.
2. Bolton-Maggs PHB, Langer JC, Iolascon A, Tittensor P, King M-J, General Haematology Task Force of the British Committee for Standards in Haematology. Guidelines for the diagnosis and management of hereditary spherocytosis - 2011 update. *Br J Haematol* 2012;156(1):37–49.
3. Makhro A, Huisjes R, Verhagen LP, et al. Red Cell Properties after Different Modes of Blood Transportation. *Front Physiol*;7.
4. Lux SE. Anatomy of the red cell membrane skeleton: unanswered questions. *Blood* 2016;127(2):187–99.
5. Satchwell TJ, Hawley BR, Bell AJ, Ribeiro ML, Toye AM. The cytoskeletal binding domain of band 3 is required for multiprotein complex formation and retention during erythropoiesis. *Haematologica* 2015;100(1):133–42.
6. Ding Y, Casey JR, Kopito RR. The major kidney AE1 isoform does not bind ankyrin (Ank1) in vitro. An essential role for the 79 NH2-terminal amino acid residues of band 3. *J Biol Chem* 1994;269(51):32201–8.
7. Barneaud-Rocca D, Etchebest C, Guizouarn H. Structural model of the anion exchanger 1 (SLC4A1) and identification of transmembrane segments forming the transport site. *J Biol Chem* 2013;288(37):26372–84.
8. Yasunaga M, Ipsaro JJ, Mondragón A. Structurally similar but functionally diverse ZU5 domains in human erythrocyte ankyrin. *J Mol Biol* 2012;417(4):336–50.
9. Bennett V. Ankyrins. Adaptors between diverse plasma membrane proteins and the cytoplasm. *J Biol Chem* 1992;267(13):8703–6.
10. Bull B, Koepke J, Simson E, van Assendelft O. Procedure for Determining Packed Cell Volume by the Microhematocrit Method; Approved Standard—Third Edition.
11. Bosch FH, Werre JM, Roerdinkholder-Stoelwinder B, Huls TH, Willekens FL, Halie MR. Characteristics of red blood cell populations fractionated with a combination of counterflow centrifugation and Percoll separation. *Blood* 1992;79(1):254–60.
12. King MJ, Behrens J, Rogers C, Flynn C, Greenwood D, Chambers K. Rapid flow cytometric test for the diagnosis of membrane cytoskeleton-associated haemolytic anaemia. *Br J Haematol* 2000;111(3):924–33.
13. King M-J, Telfer P, MacKinnon H, et al. Using the eosin-5-maleimide binding test in the differential diagnosis of hereditary spherocytosis and hereditary pyropoikilocytosis. *Cytometry B Clin Cytom* 2008;74(4):244–50.
14. Huisjes R, Satchwell TJ, Verhagen LP, et al. Quantitative measurement of red cell surface protein expression reveals new biomarkers for hereditary spherocytosis. *Int J Lab Hematol* 2018;40(4):e74–e77.

15. Da Costa L, Suner L, Galimand J, et al. Diagnostic tool for red blood cell membrane disorders: Assessment of a new generation ektacytometer. *Blood Cells, Mol Dis* 2016;56(1):9–22.
16. Lazarova E, Gulbis B, Oirschot B van, van Wijk R. Next-generation osmotic gradient ektacytometry for the diagnosis of hereditary spherocytosis: interlaboratory method validation and experience. *Clin Chem Lab Med* 2017;55(3):394–402.
17. Huisjes R, Bogdanova A, van Solinge WW, Schiffelers RM, Kaestner L, van Wijk R. Squeezing for Life – Properties of Red Blood Cell Deformability. *Front Physiol* 2018;9:656.
18. Lutz HU, Bogdanova A. Mechanisms tagging senescent red blood cells for clearance in healthy humans. *Front Physiol* 2013;4:387.
19. Perrotta S, Gallagher PG, Mohandas N. Hereditary spherocytosis. *Lancet* 2008;372(9647):1411–1426.
20. Bosch FH, Werre JM, Schipper L, et al. Determinants of red blood cell deformability in relation to cell age. *Eur J Haematol* 1994;52(1):35–41.
21. Willekens FLA, Werre JM, Groenen-Döpp YAM, Roerdinkholder-Stoelwinder B, de Pauw B, Bosman GJCGM. Erythrocyte vesiculation: a self-protective mechanism? *Br J Haematol* 2008;141(4):549–556.